https://dx.doi.org/10.24001/ijaems.3.4.14 *ISSN: 2454-1311*

Assessment of Biomass of Leaves of Water Hyacinth (Eichhornia crassipes) as Reducing Agents for the Synthesis of Nanoparticles of Gold and Silver

A.Munive-Olarte[1], G. Rosano-Ortega[2], P. Schabes-Retchkiman[3], M.S.M. Martínez-Gallegos[4], E. El Kassis[5], M. González-Pérez[6], F. Pacheco-García[7]

[1,2,5,6,7]Universidad Popular Autónoma del Estado de Puebla (UPAEP).
[3]Instituto de Física Universidad Nacional Autónoma de México (UNAM).
[4]Instituto Tecnológico de Toluca (ITT). Edo. De México.

Abstract— *Green chemistry methods for nanoparticles synthesis have implemented the valorization of renewable waste that reduces the use of chemicals and sub-products to minimize the environmental impact. Herein, we report a method to synthesize Ag and Au nanoparticles (AgNPs, AuNPs) using one of the world´s worst aquatic weeds, water hyacinth. From a reaction between a solution of AgNO3 or HAuCl4 and controlling the pH, the nanoparticles were synthesized. The optimum pH value to obtained uniform quantum dots was found to be acidic for AgNPs and neutral for AuNPs. The size was highly dependent on pH for AgNPs, a smaller size was for acidic pH, and the larger size was for basic pH, and cubic and hexagonal are the predominant structures, no dependent was observed in AuNPs, and orthorhombic is the most common form. This method was sustainable because water hyacinth is a renewable resource in all world, and their use is not being exploited in any process. The bioreduction process using water hyacinth promotes the metallic nanoparticles formation and applied standard conditions for temperature and pressure. Also, the rate of synthesis is fast.*

Keywords— Assessment of water hyacinth, green synthesis, gold nanoparticles, leaf biomass, silver nanoparticles.

I. INTRODUCTION

The study of the metal bioaccumulation/phytoremediation process in plants has revealed that metals are deposited as nanoparticles in various organs and tissues (Makarov et al., 2014). A nanoparticle is defined as a discrete particle that has a structure in the nanometer size range, usually from 1 to 100 nm. The high surface area due to volume ratio of nanoparticles makes their physicochemical properties quite different from those of the bulk material (Hebeish, El-Rafie, El-Sheikh & El-Naggar, 2013; Ahmad, 2014). Many researchers have been focused on silver and gold nanoparticles (AgNPs, AuNPs) in various fields of applications. Metal ion adsorption Bahadar et al., 2014; antimicrobial activity Muhammad et al., 2014; photocatalytic activity Wei et al., 2014; chemical sensors Rahman, Khan, Jamal, Faisal & Asiri, 2012 and, labeling Urusov et al., 2015.

Generally, AgNPs and AuNPs are synthesized by several methods whether physical or chemical. Thermal decomposition Hosseinpour & Ramezani, 2014; sonochemical Mohd & Ashokkumar, 2015; Darroudi, Zak, Muhamad, Huang & Hakimi, 2011; solvothermal Choi et al., 2013; microemulsion Ahmad, Wani, Al-Hartomy, Al-Shihri & Kalam, 2015; Jurkin, Guliš, Dražić, & Gotić, 2016; and laser ablation Urusov et al., 2015. The most of these methods need controlled environments and involve the use of hazardous chemical reagents like sodium borohydride and hydrazine hydrate (Hebeish et al., 2013). The request for an environmentally sustainable synthesis method has led to green chemistry techniques (Shameli et al., 2012). This approach could have a reduction/elimination of toxic and hazardous substances in the synthesis processes of metallic nanoparticles. Green chemistry uses microorganisms, enzymes, algae, plants (Majeed et al., 2016) and biomolecules (Hebeish et al., 2013).

The water hyacinth plants were considered as a good source in metal nanoparticles synthesis; it is contemplated as a weed because of growth in rivers and streams. It has been recognized as a hyperaccumulator organism in which high concentration of tannins makes it an excellent tool for heavy metals removal and metal nanoparticles synthesis (Rosano-Ortega et al., 2007).

https://dx.doi.org/10.24001/ijaems.3.4.14 *ISSN: 2454-1311*

Different parts of plants, such as leaves roots, stems, fruits, seeds, flowers, and latex; have been used for AgNPs and AuNPs synthesis (Rashidipour & Heydari, 2014; Mohd et al., 2015; Wang et al.,2016; Shameli et al., 2012; Babu, Aishwarya, Vidya & Saidutta, 2014; Heydari & Rashidipour,2015; Baghizadeh, et al., 2015; Baharara, Namvar, Ramezani, Hosseini, & Mohamad, 2014; Ankamwar, Gharge & Sur, 2015; Guidelli, Ramos, Zaniquelli & Baffa, 2011); Various phytochemical compounds, including terpenoids, polyphenols, sugars, alkaloids, phenolic acids, and proteins, play a major role in the bioreduction of metals (Makarov et al., 2014). Tannic acid, a polyphenolic compound, has been used as a reductant agent, in which case phenols take part in the redox reaction by forming Quinones and donating electrons that reduce oxidized metal ions to form nanoparticles (Ahmad, 2014).

Rosano-Ortega et al. (2006) proposed an application of the water hyacinth biomass for the Mn reduction from a MnSO4 solution and observed the dependence of the nanoparticle´s size as follows pH conditions, in which the smallest clusters (1-4 nm) were generated using a pH=5. Thus a change in pH gave it a modification of the chemical state (ionization) of the phytochemicals in plants, which affects their capacity to reduce metal ions (Makarov et al., 2014; Rashidipour et al., 2014).

Water hyacinth was considered as a research subject due to the following characteristics:

i). It is an aquatic weed, shared and available all over the world.

ii). Accepts polyphenolic compounds in all sections of plants; But leaves contain a greater amount of these due to the plant's defense mechanism (Rashidipour et al., 2014). Because of these characteristics, polyphenolic compounds contribute to the reduction of silver and gold ions.

iii). Also, the leaves take less time than the roots and stem in the reduction process.

For this study, a sustainable method was proposed for AgNPs and AuNPs synthesis using water hyacinth´s leaves. Also, the pH effect was evaluated to optimize the synthesis route; in the same way, composition, size, and structure of the AgNPs and AuNPs were performed by using high-resolution electron microscopy.

II. MATERIALS

Hydro chloroauric acid trihydrate ($HAuCl_4$ $3H_2O$, 99.9%) and silver nitrate ($AgNO_3$, 99.0%) was purchased from Sigma-Aldrich, buffer solutions for pH 5 and seven were obtained from MERCK and for pH 9 and 11 from HYCEL. The water hyacinth was collected from Valsequillo Reservoir, Puebla, State in Mexico. All aqueous solutions were made using try distilled water.

III. METHOD

Biomass process: Water hyacinth leaves were washed in running tap water, and received a second washing in try distilled water until it was evident. Then, the leaves were cut into small pieces and dried by solar radiation for 3h. The pieces were pulverized with a mortar and pestle and then with a blender. The obtained powder was washed with a solution of HCl 0.01N because it was required to break the cellulose, which improves the yield of sugars and release of phytochemicals, and finally it was dried again in a preheated oven at 80°C for 24h. The final powder was considered the biomass and was selected through a sieve (mesh #80) of diameter $\leq$ 0.098in.

Synthesis of nanoparticles: Silver and gold nanoparticles were obtained according to the previously described method with slight modifications (Rosano et al., 2006; Schabes et al., 2006; Canizal et al., 2006); the flow of the process is shown in Figure 1. A homogeneous suspension of biomass was prepared with a concentration of 5 mg/mL in try distilled water using an ultrasonic bath (15 min). The pH of the solution was controlled by a buffer solution to the values of 5, 7 and 9 for AgNPs and 5, 7 and 11 for AuNPs. After placing the solutions in an ultrasonic bath (15min), it was centrifuged (3000 rpm) for 30 min. Then 25 mL of a silver solution 3 x 10^{-4} M of $AgNO_3$ or gold solution 3 x 10^{-4} M of $HAuCl_4$ was added. The samples were mixed homogeneously using an ultrasonic bath (15 min) and centrifuged (3000rpm) for one h. Finally, the biomass was separated from the solution by vacuum filtration using a filter with pore size of 0.45 µm. The final settlement was kept at rest for 48 h. The process was carried out at steady conditions.

Characterization of nanoparticles: The analysis by TEM and HRTEM was carried out, using a JEOL JEM-2010F microscopy with a FasTEM for 2.3Å resolution. A couple of drops of the AgNPs or AuNPs solutions were deposited on a copper grid covered with amorphous carbon. HRTEM were obtained at various defocus conditions, including the optimal (Scherzer condition). Finally, Fast Fourier Transforms (FTT) was obtained from the images to identify the crystalline structure of each particle.

https://dx.doi.org/10.24001/ijaems.3.4.14 *ISSN: 2454-1311*

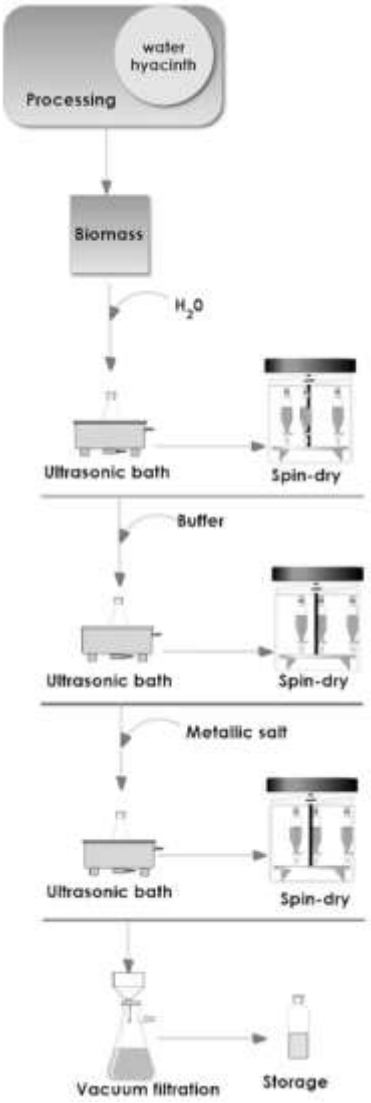

Fig.1: Schematic process of silver and gold nanoparticles synthesis with the biomass of leaves from water hyacinth.

Table captions appear centered above the table in upper and lower case letters. When referring to a table in the text, no abbreviation is used and "Table" is capitalized.

IV. RESULTS AND DISCUSSION

Particle Size Distribution (PSD). Different samples have been achieved by varying the pH value. The phytochemicals achieved with a variety of pH allowed to obtained AgNPs and AuNPs with a small size distribution and different configurations. TEM measurements were carried out to determine the size of AgNPs and AuNPs, also for both of them, in the micrographs, it was seen a trimodal size distribution (small, medium and large). Figure 2 shows the PSD for AgNPs. Here it can be observed changes in particle size due to pH value. In Figure 2a for pH= 5, a large number of nanoparticles were in 1-10 nm, for pH= 7 a great mix of particles were detected for 1-40 nm (Figure 2b) and at pH=9 the majority of nanoparticles are in 1-20 nm (Figure 2c). To confirm this behavior; in Table 1 was included the finished size for nanoparticles, 9.3 ± 7.1 nm, 21.93 ± 14.46 nm and 26.3 ± 34.66 nm for pH 5, 7 and 9 respectively. As follows these results at acidic pH small-sized nanoparticles were formed, whereas at neutral pH a large number of nanoparticles have been trained.

Table.1: Size, structure and composition of Ag and Au nanoparticles obtained with leave´s biomass of water hyacinth.

Metal	Precursor	pH	Average Size	Composition	Percent	Structure	Plane
Ag	$AgNO_3$	5	9.3±7.1	Ag^0	86%	FCC	[111], [102]
		7	21.93 ± 14.46	UD	UD	UD	UD
		9	26.3± 34.66	Ag_6O_2	80%	HP	[001]
Au	$HAuCl_4 * 3H_2O$	5	6.3± 3.3	Au^0	81%	UD	[111]
				AuO	19%	UD	UD
		7	4.2±1.79	AuO	68%	UD	UD
				Au_2O_3	32%	FCO	[133]
		11	47.8± 38	Au_2O_3	90%	UD	[511]

FCC: Face-centered cubic, HP: Hexagonal Primitive FCO: Face-centered orthorhombic. UD: Unidentified Source: Author's own elaboration.

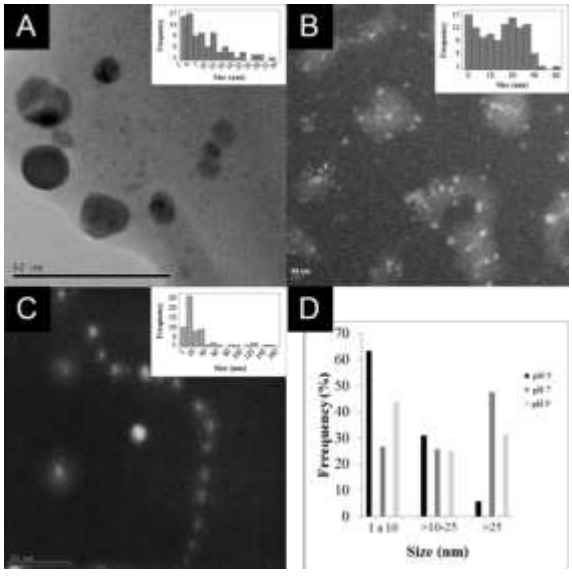

Fig.2: Low magnification electron micrographs of the Ag nanoparticles obtained at pH values: (A) 5; (B) 7; (C) 9; and the corresponding size distribution plots. The histograms show the range of particle size distribution (D).

The optimum pH was found to be 5, where over 60% of particles have sizes between 1 and 10 nm. These results are according to Baghizadeh et al. (2014), they report

https://dx.doi.org/10.24001/ijaems.3.4.14 *ISSN: 2454-1311*

optimum pH=4 to synthesized AgNPs with P. harmala seeds. However, Babu et al. (2014) using medicinal Zizyphus xylopyrus bark extract to obtain AgNPs they show surface plasmon resonance (SPR) peaks of AgNPs at neutral and alkaline conditions, which is in contrast to our results, this may be due to biomass type used.

Figure 3 shows the PSD of AuNPs, there was observed an influence by pH value, in Figures 3a and 3b the most nanoparticles were in 1-10nm with pH= 5 and 7, but in pH= 11 a majority of particles was in 20-60 nm. In Table 1 the size average was included for these nanoparticles, 6.3 ± 3.3 nm, 4.2 ± 1.79 nm and 47.8 ± 38 nm for pH 5, 7 and 11 respectively. The main result was for neutral pH in which small-sized nanoparticles and the larger number of nanoparticles were formed; this is in according to the literature (Li, Li, Wan, Xu, & Hou, 2011).

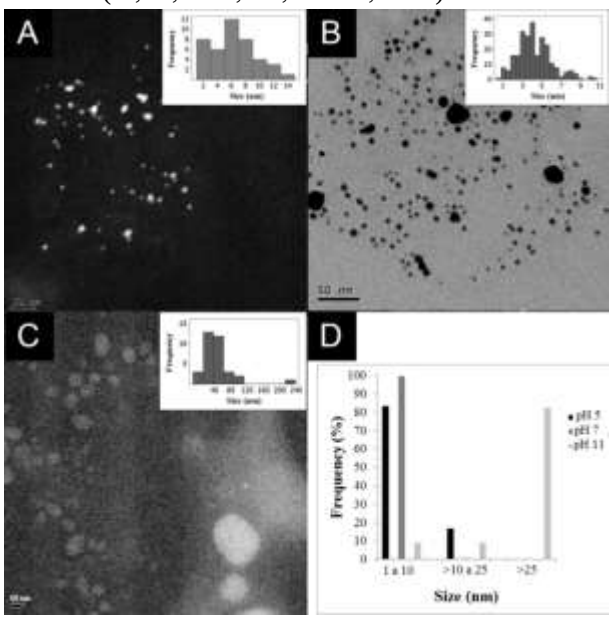

Fig.3: Low magnification electron micrographs of the Au nanoparticles obtained at pH values: (A) 5; (B) 7; (C) 11; the corresponding size distribution plots. The histograms show the range of particle size distribution (D).

HRTEM analysis. Significant results have been observed in PSD for AuNPs and AgNPs at different pH values, and the same characteristics were previously observed for other metals. (Rosano et al., 2006; Schabes et al., 2006; Canizal et al., 2006). Therefore, the optimal size distribution was obtained for AgNPs at pH=5 and for AuNPs at pH=7, where particles formed had small and regular size and symmetrical shape. Canizal et al. (2006) related the structure of the nanoparticles with the passivating agents, in this case, tannins from the biomass.

To determine the crystal arrangement formed in the AgNPs and AuNPs were analyzed HRTEM images.

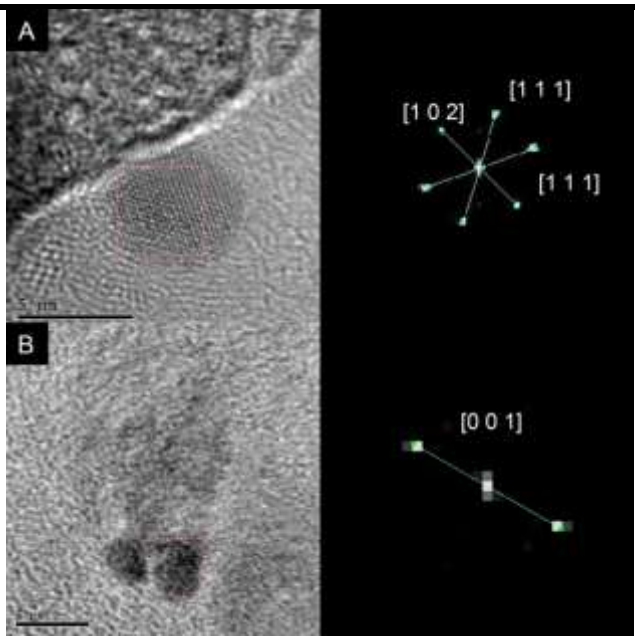

Fig.4: HRTEM images of particles observed in AgNP samples at (A) pH5 and (B) pH9, with their corresponding FFT for each image. (A) FCC nanoparticle at [111] and [102], (B) Ag_6O_2 nanoparticle at the [001] orientation.

Figure 4 shows sets of comparable images for representative structures in AgNPs samples obtained at pH 5 and 9 with their corresponding FFT. For pH= 5 (Figure 4a) it was possible to identify that 86% of nanoparticles correspond to a face-centered cubic (FCC) structure with lattice fringes having a spacing of 2.35 Å of interplanar space (JCPDS card 87-0720) and its growth preferentially over [111] and [102] planes. The rest of nanoparticles in the sample were not identified. In the case of pH = 7, the particles were formed by just a few atoms, so the contrast is not high. However, for pH = 9 (Figure 4b) it was observed that 80% of the nanoparticles corresponds to Ag_6O_2 with a hexagonal structure (HP) and lattice fringes with a spacing of 5.58 Å of interplanar space (JCPDS card 74-0878) in [001] orientation. According to with this results, it can be possible to establish, for pH=5 Ag nanoparticles were obtained, for pH=9 the silver oxide nanoparticles (Ag_6O_2) was synthesized, the results were summarized in Table 1.

Figure 5 shows sets of comparable images for representative structures for AuNPs samples obtained at pH 5, 7 and 11 and their corresponding FFT. For pH= 5 it was possible to identify two AuNPs compositions. The first one (Figure 5a) 81% of nanoparticles with lattice fringes having a 2.33 Å of interplanar space (JCPDS card 011172). It was according with the [111] d-spacing of bulk Au (Yin, Chen & Wu, 2010); the second one, 19% were of AuO (Figure 5 b) with lattice fringes having a 2.22Å of interplanar space (JCPDS card 23-0278). In the

https://dx.doi.org/10.24001/ijaems.3.4.14 *ISSN: 2454-1311*

case of the sample at pH=7 specimens, two structures were observed too.

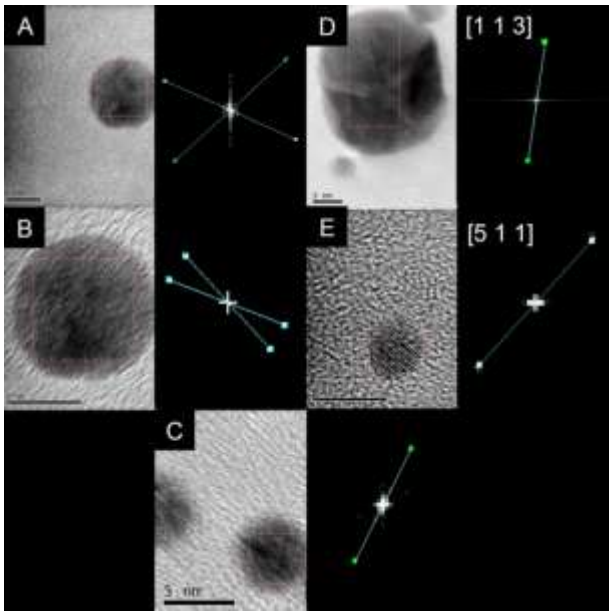

Fig.5: HRTEM images of particles observed in AuNP samples of (A & B) pH 5 and (C & D) pH 7, (E) pH 11 with their corresponding FFT for each image. (A) Au nanoparticle with [111] orientation, (B & C) AuO nanoparticles, (D) orthorhombic Au_2O_3 nanoparticle with [133] orientation, (E) orthorhombic Au_2O_3 nanoparticle with [511] orientation.

In the first one 68% of the sample corresponds to AuO nanoparticles (Figure 5c); with lattice fringes having a 2.22 Å of interplanar space (JCPDS card 23-0278). Moreover, in the second one, 32% of nanoparticles were in Au2O3 composition with a spacing of 1.19 Å (Figure 5d) corresponding to a face-centered orthorhombic (FCO) structure (JCPDS card 43-1039) in orientation [133]. Finally, for pH=11 also an Au2O3 nanoparticle in FCO structure (90%) was observed (Figure 5e) with lattice fringes having a spacing of 2.15 Å of interplanar space (JCPDS card 43-1039) on the [511] plane. According to these results, to obtain Au0 or Ag0 the best value for pH was 5, 7 respectively, while for AgNPs only one oxide was identified for particles (Table1), for AuNPs two oxides were recognized, only one configuration of gold oxide is clearly associated with pH= 11 (Au2O3). The results are condensed in Table 1.

The composition of the nanoparticle surface is intimately related to their final application because the surface will be the first aspect experiences either the environment or the organism (Christian, Von der Kammer, Baalousha & Hofmann, 2008). The metallic nanoparticles produced by biosynthesis were silver or gold oxide in the most cases, and they could be used in industrial and biomedical applications due to antimicrobial, photocatalytic, and luminescent properties.

Changes in the size distribution and structure of AgNPs and AuNPs are due to the pH varying. The AgNPs at pH= 5 was obtained the smallest size; the reduction is slow and efficient, these nanoparticles were well passivated because they search of a minimum energy surface. However, for AuNPs the smallest size was reached at pH 7, so is possibly a fast reduction process that reduces the ions faster causing aggregation and different configurations. Also, might be due to a weak passivation of tannins in the biomass with Au (Canizal, et al., 2006).

5. CONCLUSIONS

This study proposed an eco-friendly, nonhazardous, cheap, and rapid method for AgNPs and AuNPs synthesis using an invasive aquatic plant, water hyacinth, which it converts a pest to a reduction agent and a value-added chemical. The TEM analysis revealed the particle size distribution for each pH (acid, neutral or alkaline) which seems to be trimodal. For AgNPs, at pH= 5 was determined the highest percentage of nanoparticles with sizes in the range (1 a 10 nm) with a structure cubic face-centered. In the case of AgNPs, it was observed that the size and structure of nanoparticles were strongly dependent on the pH value. For AuNPs, at pH= 7 the smallest and less dispersed were obtained with two configurations (AuO and Au_2O_3). Metallic nanoparticles obtained could be applied in industry and biomedicine. Bioreduction method lets it obtained silver and gold nanoparticles, and the use of an invasive plant makes it a sustainable method to synthesize metallic nanoparticles.

REFERENCES

[1] Ahmad, T., (2014). Reviewing the Tannic Acid Mediated Synthesis of Metal Nanoparticles. Journal of Nanotechnology, 2014, 1-11, doi:10.1155/2014/954206.

[2] Ahmad, T., Wani, I. A., Al-Hartomy, O. A., Al-Shihri, A. S. & Kalam, A. (2015). Low temperature chemical synthesis and comparative studies of silver oxide nanoparticles. Journal of Molecular Structure, 1084, 9–15. doi: 10.1016/j.molstruc.2014.12.015.

[3] Ankamwar, B., Gharge, M., & Sur, U. K. (2015). Photocatalytic Activity of Biologically Synthesized Silver Nanoparticles Using Flower Extract. Advanced Science, Engineering and Medicine, 7 (6), 480-484. doi: 10.1166/asem.2015.1718.

[4] Babu, M., Aishwarya, D., Vidya, S. & Saidutta, M. B. (2014). Synthesis of silver nanoparticles using medicinal Zizyphus xylopyrus bark extract. Applied Nanoscience, 5 (6), 755-762. doi: 10.1007/s13204-014-0372-8.

[5] Baghizadeh, A., Ranjbar, S., Gupta, V. K., Asif, M., Pourseyedi, S., Karimi, M. J. & Mohammadinejad, R. (2015). Green synthesis of silver nanoparticles using seed extract of Calendula officinalis in liquid

https://dx.doi.org/10.24001/ijaems.3.4.14 *ISSN: 2454-1311*

phase. Journal of Molecular Liquids, 207, 159-163. doi: 10.1016/j.molliq.2015.03.029.

[6] Bahadar, S., Rahman, M.M., Marwani, H.M., Asiri, A. M. & Alamry, K. A. (2014). Exploration of silver oxide nanoparticles as a pointer of lanthanum for environmental. Journal of the Taiwan Institute of Chemical Engineers applications, 45 (5), 2770–2776. doi: 10.1016/j.jtice.2014.07.005.

[7] Baharara, J.; Namvar, F.; Ramezani, T.; Hosseini, N. & Mohamad, R. (2014). Green Synthesis of Silver Nanoparticles using Achillea biebersteinii Flower Extract and Its Anti-Angiogenic Properties in the Rat Aortic Ring Model. Molecules,19, 4624-4634.

[8] Canizal, G., Schabes-Retchkiman, P.S., Pal, U., Liu, H.B. & Ascencio, J.A. (2006) Controlled synthesis of Zn0 nanoparticles by bioreduction. Materials Chemistry and Physics, 97, 321–329, doi: 10.1016/j.matchemphys.2005.08.015.

[9] Choi, J., Park, S., Stojanović, Z., Han, H. S., Lee, J., Seok, H. K., Uskoković, D. & Lee, K. H. (2013). Facile Solvothermal Preparation of Monodisperse Gold Nanoparticles and Their Engineered Assembly of Ferritin–Gold Nanoclusters. Langmuir, 29 (50), 15698-15703. doi: 10.1021/la403888f.

[10] Christian, P., Von der Kammer, F., Baalousha M. & Hofmann, Th. (2008). Nanoparticles: structure, properties, preparation and behavior in environmental media. Ecotoxicology, 17, 326–343, doi: 10.1007/s10646-008-0213-1.

[11] Darroudi, M., Zak, A. K., Muhamad, M. R., Huang, N. M. & Hakimi, M. (2011). Green synthesis of colloidal silver nanoparticles by sonochemical method. Materials Letters, 66, 117–120. doi: 10.1016/j.matlet.2011.08.016.

[12] Guidelli, E. J., Ramos, A. P., Zaniquelli, M. E. D & Baffa, O. (2011). Green synthesis of colloidal silver nanoparticles using natural rubber latex extracted from Hevea brasiliensis. Spectrochimica Acta Part A: Molecular and Biomolecular Spectroscopy. 82(1), 140-145. doi:10.1016/j.saa.2011.07.024.

[13] Hebeish, A., El-Rafie, M. H., El-Sheikh, M. A., & El-Naggar, E. (2013). Nanostructural Features of Silver Nanoparticles Powder Synthesized through Concurrent Formation of the Nanosized Particles of Both Starch and Silver. Journal of Nanotechnology, 2013 (201057), 1-10.doi:10.1155/2013/201057.

[14] Heydari, R., & Rashidipour, M. (2015). Green Synthesis of Silver Nanoparticles Using Extract of Oak Fruit Hull (Jaft): Synthesis and In Vitro Cytotoxic Effect on MCF-7 Cells. International Journal of Breast Cancer, 2015 (846743), 1-6. doi:10.1155/2015/846743.

[15] Hosseinpour, S. M. & Ramezani, M. (2014). Silver and silver oxide nanoparticles: Synthesis and characterization by thermal decomposition. Materials Letters, 130, 259–262. doi: 10.1016/j.matlet.2014.05.133.

[16] Jurkin, T., Guliš, M., Dražić, G. & Gotić, M. (2016). Synthesis of gold nanoparticles under highly oxidizing conditions. Gold Bull, 49, 21-33. doi: 10.1007/s13404-016-0179-3.

[17] Li, C., Li, D., Wan, G., Xu, J. & Hou, W. (2011). Facile synthesis of concentrated gold nanoparticles with low size-distribution in water: temperature and pH controls. Nanoscale Research Letters, 6(440), 1-10. doi: 10.1186/1556-276X-6-440.

[18] Majeed, A., Ullah, W., Anwar, A. W., Shuaib, A., Ilyas, U., Khalid, P., Mustafa, G., Junaid, M., Faheem, B., & Ali, S. (2016). Cost-effective biosynthesis of silver nanoparticles using different organs of plants and their antimicrobial applications: A review. Materials Technology, 0(0), 1-8. doi:10.1080/10667857.2015.1108065.

[19] Makarov, V. V. , Love, A. J., Sinitsyna, O. V. , Makarova, S. S., Yaminsky, I. V, Taliansky, M. E. & Kalinina, N. O.(2014). "Green" Nanotechnologies: Synthesis of Metal Nanoparticles Using Plants. Acta Naturae, 6(1), 35-44,

[20] Mohd, N. S. & Ashokkumar, M. (2015). Sonochemical Synthesis of Gold Nanoparticles by Using High Intensity Focused Ultrasound. ChemPhysChem, 16 (4), 775–781. doi: 10.1002/cphc.201402697.

[21] Muhammad, A., Sadaf, H., Asghar, A., Farooq, A., Shaukat, A. S., Imran, S., Aqdas, Y., Sara, H., Safyan, A. K., & Rahman, S. (2014). Green Synthesis of Silver Nanoparticles: Structural Features and In Vivo and In Vitro Therapeutic Effects against Helicobacter pylori Induced Gastritis. Bioinorganic Chemistry and Applications, 2014 (135824), 1-11. doi:10.1155/2014/135824.

[22] Rahman, M. M., Khan, S. B., Jamal, A., Faisal, M., & Asiri, A. M. (2012). Highly sensitive methanol chemical sensor based on undoped silver oxide nanoparticles prepared by a solution method. Microchimica Act, 178 (1), 99–106. doi: 10.1007/s00604-012-0817-2.

[23] Rashidipour, M. & Heydari, R. (2014). Biosynthesis of silver nanoparticles using extract of olive leaf: synthesis and in vitro cytotoxic effect on MCF-7 cells. Journal of Nanostructure in Chemistry, 4(112), 1-6. doi: 10.1007/s40097-014-0112-3.

[24] Rosano-Ortega, G., Schabes-Retchkiman, P., Zorrilla, C., Liu, H.B., Canizal, G., Avila, P., & Ascencio, J. A. (2006). Synthesis and Characterization of Mn Quantum Dots by Bioreduction with Water Hyacinth. Journal of

https://dx.doi.org/10.24001/ijaems.3.4.14 *ISSN: 2454-1311*

Nanoscience and Nanotechnology, 6, 1-5. doi:10.1166/jnn.2006.061.

[25] Rosano-Ortega, G., Avila-Pérez, P., Zavala, G., Santiago, P., Canizal, G., & Ascencio, J. A. (2007). Inorganic Nanoparticles Induced Naturally in Water Hyacinth: Structural and Chemical Study. Journal of Bionanoscience, 1, 51–59. doi: 0.1166/jbns.2007.001

[26] Schabes-Retchkiman, P. S, Canizal, G, Herrera-Becerra, R., Zorrilla, C., Liu, H. B. Ascencio, J.A. (2006) Biosynthesis and characterization of Ti/Ni bimetallic nanoparticles. Optical Materials, 29, 95–99. doi:10.1016/j.optmat.2006.03.014.

[27] Shameli, K.; Ahmad, M. B.; Al-Mulla, E. A. J.; Ibrahim, N. A.; Shabanzadeh, P.; Rustaiyan, A.; Abdollahi, Y.; Bagheri, S.; Abdolmohammadi, S.; Usman, M. S.& Zidan, M. (2012). Green Biosynthesis of Silver Nanoparticles Using Callicarpa maingayi Stem Bark Extraction. Molecules, 17(1), 8506-8517, doi: 10.3390/molecules17078506.

[28] Suman, T.Y, Rajasree, S.R, Kanchana, A. & Elizabeth, S. B. (2013). Biosynthesis, characterization and cytotoxic effect of plant mediated silver nanoparticles using Morinda citrifolia root extract. Colloids and Surfaces B: Biointerfaces, 106, 74-78, doi: 10.1016/j.colsurfb.2013.01.037.

[29] Urusov, A. E., Petrakova, A. V., Kuzmin, P. G., Zherdev, A. V., Sveshnikov, P. G., Shafeev, G. A. & Dzantiev, B. B. (2015). Application of gold nanoparticles produced by laser ablation for immunochromatographic assay labeling. Analytical Biochemistry, 491, 65–71. doi: 10.1016/j.ab.2015.08.031.

[30] Wang, L., Xu, H., Gu, L., Han, T. T., Wang, S. & Meng, F. B. (2016). Bioinspired synthesis, characterization and antibacterial activity of plant-mediated silver nanoparticles using purple sweet potato root extract. Materials Technology, 31(8), 437-442. doi:10.1080/10667857.2015.1105575.

[31] Wei, J., Xiaoyan, W., Zhaomei, W., Xiaoning, Y., Shaojun, Y., Houfang, L. & Bin, L. (2015). Silver Oxide as Superb and Stable Photocatalyst under Visible and Near-Infrared Light Irradiation and Its Photocatalytic Mechanism. Industrial &Engineering Chemistry Research, 54 (3), 832–841. doi: 10.1021/ie503241k.

[32] Yin, X., Chen, S. & Wu, A. (2010). Green chemistry synthesis of gold nanoparticles using lactic acid as a reducing agent. Micro & Nano Letters, 5, 270–273, doi: 10.1049/mnl.2010.0117.